Auxin promotion of seedling growth via ARF5 is dependent on the

brassinosteroid-regulated transcription factors BES1 and BEH4

Anahit Galstyan[1, a] and Jennifer L Nemhauser[1¥]

[1] Department of Biology, University of Washington, Seattle, WA 98195-1800, USA.

[a] Present address: Max Planck Institute for Plant Breeding Research, Carl-von-Linné-Weg 10, 50829, Cologne, Germany.

¥ Correspondence: jn7@uw.edu

Abstract

Seedlings must continually calibrate their growth in response to the environment. Auxin and brassinosteroids (BRs) are plant hormones that work together to control growth responses during photomorphogenesis. We used our previous analysis of promoter architecture in an auxin and BR target gene to guide our investigation into the broader molecular bases and biological relevance of transcriptional co-regulation by these hormones. We found that the auxin-regulated transcription factor AUXIN RESPONSIVE FACTOR 5 (ARF5) and the brassinosteroid-regulated transcription factor BRI1-EMS-SUPPRESOR 1/BRASSINOZOLERESISTANT 2 (BES1) co-regulated a subset of growth promoting genes via conserved bipartite *cis*-regulatory elements. Moreover, ARF5 binding to DNA could be enriched by increasing BES1 levels. The evolutionary loss of bipartite elements in promoters results in loss of hormone responsiveness. We also identified another member of the BES1/BZR1 family called BEH4 that acts partially redundantly with BES1 to regulate seedling growth. Double mutant analysis showed that BEH4 and not BZR1 were required alongside BES1 for normal auxin response during early seedling development. We propose that an ARF5-BES1/BEH4 transcriptional module acts to promote growth via modulation of a diverse set of growth-associated genes.

Introduction

20

21   Plants must adapt their form to survive a complex and changing environment. The

22   extensive molecular interplay between external (i.e., light and temperature) and internal (i.e.,

23   circadian clock) signals allows for a high degree of developmental plasticity. Light-directed

24   seedling growth (photomorphogenesis) is one of the best-characterized examples of a highly

25   dense regulatory network. Small molecule hormones are critical for relaying information about

26   the light environment, as well as a diverse set of additional metabolic, environmental and

27   developmental cues [1,2]. Hormones like auxin and brassinosteroids (BRs) play a central role in

28   coordinating growth during photomorphogenesis.

29   Plants with defective responses to auxin or BRs show an array of phenotypes of light-

30   grown plants even when grown in the dark [3]. The signaling pathways downstream of auxin and

31   BRs are distinct. Auxin binds to the TRANSPORT INHIBITOR RESPONSE 1/AUXIN

32   SIGNALING F-BOX 1–5 (TIR1/AFB) family of F-box receptors and triggers the ubiquitination

33   and degradation of AUXIN/INDOLE-3-ACETIC ACID (Aux/IAA) co-repressors. Loss of the

34   Aux/IAAs activates AUXIN RESPONSE FACTORs (ARFs) to regulate gene expression [4–6].

35   ARFs bind to an auxin response element (AuxRE, TGTCTC) and related *cis*-elements in target

36   promoters [7–11]. In contrast, BRs bind and activate the BRASSINOSTEROID-INSENSITIVE1

37   (BRI1)-associated receptor complex at the plasma membrane. A phospho-relay cascade

38   culminates in dephosphorylated and nuclear-localized transcription factors, including BRI1-

39   EMS-SUPPRESOR1/ BRASSINOZOLERESISTANT2 (BES1/BZR2, hereafter BES1) and

40   BZR1 [12–14]. BES1 and BZR1 regulate gene expression by binding to both E-box (CANNTG)

41   and BRRE (CGTG(T/C)G) *cis*-elements in target promoters [15,16].

42   Genetic, physiological, and genomic analyses demonstrate molecular and physiological

43   responses of auxin and BRs are interdependent. BRs promote auxin transport, hence altering

44   overall auxin distribution within the plant [17,18]. BRs also regulate expression of genes

45   involved in the core auxin response [19–21] and a BR-regulated kinase targets members of the

46   ARF family [22–25]. Auxin stimulates *de novo* BR biosynthesis by directly regulating

47   expression of *DWARF4* (DWF4), a BR biosynthetic enzyme [26,27]. BRI1 is a direct target of

48   activator ARF5/MONOPTEROS (hereafter, ARF5) [28]. In addition ARF6 and ARF7 were

49   shown to interact with BZR1 to regulate shared target genes [29].   Previously, we demonstrated

50   that a bipartite element in the promoter of *SAUR15* gene that includes a type of E-box called a

51   HUD element (CACATG) and a variant of the AuxRE (TGTCT) are bound by ARF5 and BES1,

52   and that binding by both transcription factors is required for induction of expression by either

53   hormone [30]. In this work, we expanded this study to include other growth-associated genes

54   with predicted bipartite elements in their promoters. We found that BES1 sensitizes hypocotyl

55   response to auxin by enhancing ARF5 binding to shared target promoters. The evolutionary loss

56   of the conserved promoter architecture with bipartite elements results in loss of hormone

57   responsiveness. BEH4, a previously uncharacterized paralog of BES1, was found to act

58   redundantly with BES1 as a major regulator of seedling growth. We propose a model where

59   shared promoter architecture facilitates a coordinated and highly responsive growth controlling

60   module encompassing genes from diverse families.

61

62   **Materials and Methods**

63   **Plant materials and growth conditions**

64   The wild type is Arabidopsis thaliana ecotype Col-0 except *beh1-2* and *beh2-1* that are in Col-3

65   background. *bes1-D* [12], *bzr1-D* [58], *bin2-D* [59], *lng1-3* [46], *xth17* [52], *pif7-2* [60],

66   ARF5$_{PRO}$::ARF5:GFP [31], BES1$_{PRO}$::BES1:GFP [12], XTH19$_{PRO-1.1kb}$::GUS and XTH19$_{PRO-}$

67    $_{0.3kb}$::GUS [34] were previously described. Single T-DNA insertion lines: *bes1-2* (WiscDsLox

68   246D02), *bzr1-2* (GABI-Kat 857E04), *beh1-2* (SAIL_40_D04, Col-3 background), *beh2-1*

69   (SAIL_76_B06, Col-3 background), *beh3-1* (SALK_017577), *beh4-1* (SAIL_750_F08) and

70   double mutants: *bes1-2beh4-1* and *bes1-2bzr1-2* are described lines [33]. For detailed

71   information on genotyping methods, primers and generation of double mutants see

72   Supplementary data.

73   For seed production and crosses, plants were grown in a growth chamber under LD conditions.

74   Seeds were surface sterilized (20 min in 70% ethanol, 0.01% Triton X-100, followed by a rinse

75   in 95% ethanol) for all the physiological and molecular analyses. For hypocotyl and GUS assays,

76   sterilized seeds were suspended in water and sown individually on plates containing 0.5x

77   Linsmaier and Skoog (LS) (LSP03, Caisson Laboratories, Inc., http://www.caissonlabs.com/)

78   with 0.8% phytoagar (40100072-1, Plant Media: bioWorld, http://www.plantmedia.com/), and

79   stratified in the dark at 4°C for 3 days. Plates were placed vertically in a Percival E-30B growth

80   chamber set at 20°C in 30 µmol m^{-2} s^{-1} of photosynthetically active radiation white light with

81   short-day conditions (8 h light, 16 h dark). For gene expression and ChIP assays, sterilized seeds

82   were suspended in 0.1% agar (BP1423, Fisher Scientific, http://www.fisher.co.uk/), spotted on

83   plates containing 0.5x LS with 0.8% phytoagar, stratified in the dark at 4°C for 3 days and grown

84   horizontally as described above.

85   **Chemical treatments**

86   To prepare stock solutions brassinosteroid (brassinolide, 101, Chemiclones, Inc.,

87   www.chemiclones.com), IAA (705490, PlantMedia.com) and picloram (P5575, Sigma) were

88   dissolved in dimethyl sulfoxide and diluted directly into plate medium to 1µM/0,5µM, 50µM

89   and 5µM concentration respectively. Stock solutions were kept at –20ºC until use.

90   **Accession numbers**

91   Sequence data from this article can be found in the Arabidopsis Genome Initiative or

92   GenBank/EMBL databases under the following accession numbers: *BES1* (At1g19350), *BZR1*

93   (At1g75080), *BEH1* (At3g50750), *BEH2* (At4g36780), *BEH3* (At4g18890), *BEH4* (At1g78700),

94   *ARF5* (At1g19850), *IAA6* (At1g52830), *XTH14* (At4g25820), *XTH17* (At1g65310), *XTH18*

95   (At4g30280), *XTH19* (At4g30290), *XTH26* (At4g28850), *XTH31* (At3g44990), *XTH32*

96   (At2g36870), *LNG1* (At5g15580), *PIF7* (At5g61270), *ACT2* (At3g18780)and housekeeping

97   gene-HK (At1g13320).

98   **Hypocotyl measurements**

99   Seedlings were grown vertically on square plates with 0.5xLS media supplemented with 80%

100   ethanol (mock), 5µM picloram or 0.5µM BL under abovementioned conditions. Plates were

101   scanned using EPSON Perfection V5000 scanner every 24h 2 days after germination. Generated

102   images were used to measure hypocotyl length. The National Institutes of Health ImageJ

103   software (rsb.info.nih.gov) was used on digital images to measure the length of different organs

104   of the seedlings, as indicated elsewhere [61]. At least 15 seedlings were used for each data point,

105   experiments were repeated 3-5 times and a representative one is shown. Statistical analyses of

106   the data (T-test and two-way ANOVA) were performed using GraphPad Prism version 4.00 for

107   Windows (www.graphpad.com).

108   **Gene expression analysis by RT-qPCR**

109   Seedlings were grown vertically on 0.5xLS plates under abovementioned conditions. Expression

110   analyses were performed on seedlings collected at dawn on day 7 (D8) grown in SD. Only the

111   expression analysis of BES1-BZR1-BEH family members in single mutants was performed on

112   dark grown 7-day-old seedlings (D8). Hormone treatments were done 3h prior to collection in

113   liquid 0.5x LS media supplemented with equal volumes of 80% ethanol (mock), IAA (to final

114   concentration 50µM) or BL (to final concentration 1µM). All samples were immediately frozen

115   in liquid nitrogen and stored at -80°C until processing. Total RNA was extracted from 100 mg of

116   whole seedling tissue using the Spectrum Plant Total RNA Kit (Sigma, STRN50), treated with

117   DNaseI on columns (Qiagen, DNASE70) and lµg of eluted RNA was used for complementary

118   DNA (cDNA) synthesis using iScript (Bio-Rad, 170-8891). Samples were analyzed using SYBR

119   Green Supermix (Bio-Rad, 170-8882) reactions run in a CFX96 Optical Reaction Module (Bio-

120   Rad). Expression for each gene was calculated using the formula [62] (E_{target})–ΔCP_{target}

121   (control-sample)/(E_{ref})–ΔCP_{ref} (control-sample) and normalized to a reference housekeeping

122   gene (At1g13320). Primer for RT-qPCR analysis were designed by QuantPrime program. Primer

123   sequences are listed in Table S2.

124   **GUS staining**

125   7-day-old (D8) seedlings were treated with mock (80% ethanol), 50µM IAA and 1µM BL in

126   liquid 0.5xLS on plate and collected after 3h, similar to sample preparation for RT-qPCR. GUS

127   staining was performed as previously described [63] using 1mM Ferri/Ferro concentration for

128   1.5h at 37°C in the dark. Seedlings were mounted on glass slides in 50% glycerol. Images were

129   taken using Leica microscope and whole seedling images were reconstructed using MosaicJ

130   feature of Fiji plugin from National Institutes of Health ImageJ software (rsb.info.nih.gov).

131   **ChIP assay**

132   Seven-day-old (D8) seedlings (BES1$_{PRO}$::BES1:GFP , ARF5$_{PRO}$::ARF5:GFP and *bes1-D* x

133   ARF5$_{PRO}$::ARF5:GFP) were treated for 3h with 80% ethanol (mock) or 50µM IAA in liquid

134   0.5xLS media on plate and crosslinked in 1% formaldehyde under vacuum on ice. Cross-linking

135   was stopped by infiltrating in 0.125M room temperature glycine solution. Seedlings were

136   subsequently frozen in liquid nitrogen and ground to a fine powder with mortar and pestle.

137   Samples were resuspended in nuclei extraction buffer [0.25 M Suc, 100 mM MOPS, pH 7.6, 10

138   mM MgCl2, 5% Dextran T-40, 2.5% Ficoll, 20 mM b-mercaptoethanol, and mini-Complete

139   Proteinase Inhibitor tablet (Roche Applied Science, 04693124001)], filtered through Miracloth

140   (Calbiochem, 475855), and centrifuged to collect nuclei. Nuclei were lysed with Nuclei lysis

141   buffer (50 mM Tris- HCl, pH 8, 10 mM EDTA, and 1% SDS). ChIP dilution buffer was added

142   (1.1% Triton X-100, 1.2 mM EDTA, 16.7 mM Tris, pH 8.0, 167 mM NaCl, and 0.01% SDS),

143   and chromatin was fragmented using Biorupter sonicator (Fisher Scientific, Bioruptor® UCD-

144   200). An aliquot of fragmented chromatin served as an input control for qPCR analysis, and the

145   remainder was subjected to immunoprecipitation. Dynabeads protein A (Invitrogen, 100-02D)

146   coupled with anti-GFP (Ab290, Abcam) antibody were used to enrich for ARF5$_{PRO}$::ARF5:GFP

147   or BES1$_{PRO}$::BES1:GFP containing chromatin fragments. Samples were washed and eluted off

148   of Dynabeads using nuclei lysis buffer, and cross-links were reversed by incubating with 300

149   mM NaCl. DNA was purified using a PCR clean-up kit (Qiagen, 28104). Low Adhesive

150   Dnase/RNase free tubes (Bioplastics, B74030) were used for all the procedures. ChIP-qPCR

151   assay data was normalized to housekeeping gene (At1g13320) coding sequence, and results are

152   expressed as ratios of qPCR signal to the antibody IP of wild-type samples (Figure 1) or IP

153   without antibody in reporter lines (Figure S1). ChIP-qPCR results represent the average of at

154   least 2-4 independent biological replicates. Primers for ChIP-qPCR analysis are listed in

155   Supplemental Table S2.

156

157   **Results**

158   **BES1 sensitizes hypocotyl to exogenous application of auxin**

159   BRs enhance seedling sensitivity to auxin [22]. To test the extent to which this effect of BR on

160   auxin response is mediated by BES1, we exposed seedlings with wild-type or constitutively

161   active BES1 to the synthetic auxin picloram (Figure1A). As previously described, *bes1-D*

162   hypocotyls were longer than those of wild-type seedlings (Figure 1A; [13]); however, the

163   application of synthetic auxin, picloram, strongly exaggerated the difference in hypocotyl length

164   between *bes1-D* mutant and wild-type plants. Based on previous results using the *SAUR15*

165   promoter [30], we hypothesized that increased BES1 activity led to auxin hypersensitivity by

166   enhancing DNA binding of ARF5 to promoters with bipartite-type *cis*-elements.

167

168   Using the large list of BES1 targets generated by ChIP-seq and microarray analysis [16], we

169   focused on the subset of targets with putative bipartite elements in their promoters. Ten genes

170   were selected based on the following criteria: being targets of ARF5 or BES1 [16,31], having

171   evidence of their expression regulated by auxin or BRs [21,32], and functional information

172   and/or mutant phenotypes. We validated these candidate genes and the bipartite elements in their

173   promoters with ChIP assays in the previously characterized ARF5$_{PRO}$::ARF5:GFP [31] and

174   BES1$_{PRO}$::BES1:GFP [12] lines. From our initial list, *XYLOGLUCAN*

175   *ENDOTRANSGLUCOSYLASE/HYDROLASE 19* (*XTH19*), *INDOLE-3-ACETIC ACID 6 (IAA6)*,

176   *LONGIFOLIA1 (LNG1)* and *PHYTOCHROME-INTERACTING FACTOR7 (PIF7)* were found to

177   be the strongest candidates for further analysis (Figure S1). To test whether BES1 enhances

178   DNA-binding of ARF5, we crossed ARF5$_{PRO}$::ARF5:GFP line to *bes1-D* mutant. Increased

179   BES1 activity did increase DNA binding by ARF5 in most cases (Figure 1B).

180

181   **BES1 and BEH4 are major regulators of BR responses in seedling stage**

182   BES1 belongs to a family of six genes [13], with BES1 and BZR1 the best-characterized

183   members [15,16]. BEH1-4 undergo BR-induced phosphorylation status changes similar to BES1

184   and BZR1 [13]. The functional redundancy of this transcription family was documented recently

185   in trait robustness [33], however their role in BR pathways remains poorly understood. BEH4,

186   the most recent member of the family, acts redundantly with BES1 to regulate hypocotyl length

187   in skotomorphogenic seedlings [33]. To investigate whether other members of the

188   BES1/BZR1/BEH gene family contribute to auxin sensitivity, we analyzed T-DNA insertion

189   alleles for each member of the BES1/BZR1/BEH family [33]. In these T-DNA insertion lines,

190   we measured hypocotyl elongation in the absence or presence of BL or picloram. Hypocotyl

191   response to BL was modestly reduced only in *bes1-2*, *bzr1-2* and *beh4-1* single mutants (Figure

192   S2), while the response to picloram was not affected significantly in any of single mutants

193   (Figure S3). Based on these findings, we selected *bes1-2 beh4-1* and *bes1-2 bzr1-2* double

194   mutants for further investigation. *bes1-2 beh4-1* double mutants are dwarfs that resemble known

195   mutants with compromised BR synthesis or signaling (Figure 2A). They also show dramatically

196   reduced response to BL and significantly reduced response to picloram (Figures 2B and C). In

197   addition, rosettes of *bes1-2 beh4-1* resembled *bin2-D* mutants where activity of the entire

198   BES1/BZR1/BEH family should be suppressed (Figure 2A). In contrast, *bes1-2 bzr1-2* double

199   mutants had an essentially wild-type response to picloram, but significant reduction in BR

200   sensitivity (Figure S4).

201

202   **BES1 status affects bipartite gene expression**

203   We used RT-qPCR to investigate the effect of BES1 on bipartite target gene expression (*XTH19*,

204   *IAA6*, *LNG1* and *PIF7*). Single mutants of *bes1-2* and *beh4-1* did not have significant effect on

205   target gene expression (Figure S5), consistent with their weak physiological phenotypes (Figures

206   S2 and S3). However, in *bes1-2 beh4-1* double mutant the expression of *XTH19* and *IAA6* was

207   attenuated, and the expression of *LNG1* was modestly decreased. In contrast, the expression of

208   *PIF7* was induced in the double mutant. As expected, in *bes1-D* the opposite tendencies were

209   observed for all genes (Figures 3A). Both BR and auxin dramatically induced the expression of

210   *XTH19* and *IAA6*; while both hormones modestly repressed the expression of *PIF7* (Figure 3B).

211   The hormone responsiveness of those genes was affected by BES1/BEH4 status (Figure 3C).

212

213   We further investigated the role of bipartite target genes in BR and auxin induced elongation

214   responses. We analyzed single knockout alleles of *xth17*, *lng1-3* and *pif7-2*. Since *XTH19* had no

215   available loss-of-function mutant, we analyzed a mutant in *XTH17*, part of the same *XTH17-20*

216   gene cluster whose members act redundantly with one another [34,35]. *XTH17* promoter also

217   carried a conserved bipartite element, and its expression followed a similar pattern as *XTH19* in

218   our RT-qPCR analysis (Figure 4B). The hypocotyls of all three mutants tended to be shorter than

219   those in wild-type seedlings in control (mock) conditions. In the presence of picloram, these

220   effects became more obvious (Figure 3D).

221

222 **Evolutionary conservation of bipartite elements predicts hormone responsiveness of**

223 **promoters**

224 *XTH19*, *IAA6* and *LNG1*, as well as the previously characterized bipartite target gene *SAUR15*,

225 belong to large gene families. In the case of *XTH19*, we observed that the expression of at least

226 three genes in the same clade (*XTH17-19*) were similarly affected by BES1, as well as treatment

227 with BR or auxin (Figures 4B and C). We reasoned that these similar transcriptional patterns

228 across paralogs might be due to shared promoter architecture. Previously, it was documented that

229 *XTH17-20* cluster has a specific motif conservation within the promoter region [34]. We found

230 that this conserved motif includes the bipartite element we found in *XTH19* promoter (Figure

231 4A). Similar promoter architecture is also observed for group of so-called *SAUR* class 2 and 3

232 that are expressed in hypocotyls [36]. 17 out of 30 genes in this group harbor bipartite elements

233 within 250bp upstream of the transcription start, and all of these have been shown to be regulated

234 by BR and auxin (Table S1). We predicted that the absence of bipartite element would

235 compromise hormone responsiveness of target genes. In fact, no hormonal responses to either

236 BL or IAA was observed for several *XTHs* closely related to *XTH17-19* cluster, such as *XTH14*,

237 *31* and *32*, in which either HUD or AuxRE elements were lost. *XTH31* expression was still

238 responsive to BL, likely due to a retained HUD element at -900bp. *XTH26* has conserved

239 bipartite element and was included as a positive control. Despite its low expression levels,

240 *XTH26* was repressed by both hormones.

241

242 In previous work focused on characterization of the *XTH17-20* cluster, Vissenber and colleagues

243 generated a set of transgenic lines of promoter truncations fused to GUS. We tested full-length

244 (XTH19$_{PRO-1.1kb}$::GUS) and 300bp (XTH19$_{PRO-0.3kb}$::GUS) truncated promoter reporter lines in

245 our conditions. Seedlings of full-length XTH19$_{PRO-1.1kb}$::GUS line exhibited weak staining in the

246 hypocotyl area and root tip in control (mock) conditions, 3h of IAA and BL treatment intensified

247 the blue staining specifically in hypocotyl and petiole tissues. Interestingly the XTH19$_{PRO-}$

248 $_{0.3kb}$::GUS truncation, in which a portion of the bipartite elements is deleted, completely

249 abolished reporter gene expression and hormone responsiveness (Figure S6). These data suggest

250 that bipartite elements in *XTH19* promoter are important for its proper expression level, pattern

251 and hormone-sensitivity.

252

Discussion

254 During photomorphogenesis, seedling growth is shaped by a complex interacting networks of

255 plant hormones to insure the seedling architecture and growth are synchronized to environmental

256 conditions. In this study, we provide molecular mechanism for how two well-characterized

257 regulators of photomorphogenesis, auxin and BRs, converge in a tunable bipartite transcriptional

258 module to promote growth.

259

260 We have shown that BES1 and BEH4, but not BZR1, play a major role in BR and auxin

261 responsiveness in young seedlings. These results are consistent with a recent study that found

262 that BEH4 acts redundantly with BES1 in controlling hypocotyl length robustness in dark-grown

263 seedlings [33]. BES1 is also temperature sensitive, a trait regulated by auxin [37,38]. It is likely

264 that other family members, such as BZR1, play growth-promoting roles at other stages or under

265 other conditions. Consistent with this hypothesis, ChIP-seq analyses of BES1 and BZR1,

266 performed in two-weeks old seedlings and leaves of adult plants, respectively, found a large

267 overlap in target promoters [15,16]. BES1 and BZR1 show differential interaction with the

268   chaperone HSP90 [37] which may facilitate interactions with distinct cell type- or stage-specific

269   partners.

270

271   Cooperative binding and activity of BR-regulated transcription factors appear to be a recurrent

272   motif in plant signaling. Our group previously found that the interaction between auxin and BR

273   relies on two cis-elements, a bipartite element that contains AuxRE and HUD-type E-box

274   elements bound by ARF5 and BES1, respectively [30]. Here, we show that specific mutations of

275   E-boxes/AuxRE elements during evolution or disruption of bipartite target XTH19$_{PRO}$ had direct

276   effect on gene expression level and patterns (Figure 5 and S6). A similar mechanism of

277   cooperative binding has been proposed for BZR1 and ARF6 [29]. BES1 also interacts with the

278   bZIP transcription factors HAT1 and HAT3 to co-repress the BR biosynthetic gene *DWF4* [39].

279   In addition, both BES1 and BZR1 interact with the bHLH transcription factor PIF4 and bind to

280   E-box elements to co-activate target promoters [40].

281

282   Target genes with bipartite promoters identified in this study are known regulators of plant

283   growth. *IAA6*, also called *SHORT HYPOCOTYL1*, encodes a co-repressor of auxin signaling that

284   is also involved in negative feedback [41]. PIF7 is as major regulator of shade responses that

285   directly induces auxin biosynthesis genes such as members of the *YUCCA* family [42]. Dominant

286   *iaa6/shy1-1D* and loss-of-function *pif7* mutants exhibit short hypocotyl phenotypes [43,44]

287   (Figure 3D). *LNG1* encodes a protein localized to cortical microtubules (cMT) [45] that was

288   initially identified as a dominant mutant with exaggerated elongation of petioles via

289   unidirectional cell elongation [46,47].

290

291   The switch between different cMT orientations can be triggered by various endogenous and

292   exogenous signals that are known to modulate growth, including light and various hormones

293   [48–50]. Actin and cMT proper orientation and localization are required for both auxin and BR-

294   mediated cell elongation [51–53]. In addition, Sasidharan and colleagues demonstrated that

295   genetic and pharmacological disruption of cMTs affects a shade-specific subset of *XTH* genes

296   (*XTH17* and *XTH19*) expression as a result of auxin re-distribution [52]. XTHs, similar to

297   expansins, are cell wall modifiers that induce cell expansion. Overexpression of *XTH18, XTH19*

298   and *XTH20* (all part of the bipartite *XTH* clade) stimulated hypocotyl growth in early

299   developmental stage of Arabidopsis seedlings [35], while similarly loss-of-function of *XTH17*

300   results in inhibition of hypocotyl growth (Figure 3D). In addition, the functionally redundant

301   *LNG3* and *LNG4* genes regulate turgor-driven polar cell elongation through activation of *XTH17*

302   and *XTH24* [54]. BES1/BZR1 and PIFs were also implicated in hypocotyl elongation during

303   thermomorphogenesis via regulation of *LNG1* and *LNG2* [55–57]. We found that *LNG1* and

304   *XTH19* are bipartite targets of the ARF5-BES1/BEH4 module rapidly induced by both auxin and

305   BRs (Figures 3 and 4) further connecting reorientation of cMTs and cell wall loosening.

306

307   We propose that the ARF5-BES1/BEH4 transcriptional hub rapidly and coordinately modulates

308   a suite of growth control genes (Figure 6). This module can serve as an integration point for

309   external signals such as shade and temperature to tune internal growth program and adjust it to a

310   changing environment. For example, exposure to shade could rewire this growth network by

311   increasing the expression/activity of bHLH transcription factors that interact with BES1, and, in

312   this way, change the composition and thereby the targets of the auxin/BR transcriptional

313   complex. Future studies are needed to fully understand how each potential transcriptional

314   complex impacts target gene selectivity and growth dynamics in a tissue- and developmental

315   stage-specific manner.

316

317   **Acknowledgements**

318   This work was supported by the National Institutes of Health (R01-GM107084). We thank Dr.

319   Jennifer Lachowiec and Dr. Christine Quietsch for providing seed stocks before publication, as

320   well as Dr. Dolf Weijers, Dr. Zhi-Yong Wang, Dr. Peter Quail, Dr. Kazuhiko Nishitani, Dr.

321   Ronald Pierik and Dr. Jaime F Martinez-Garcia for sharing published resources.

322

323   **Authors Contribution**

324   AG and JLN conceived and designed the experiments. AG collected and analyzed the data, as

325   well as preparing the figures. AG and JLN wrote the manuscript.

326

327   **Supporting Information**

328   **Figure S1:** BES1 and ARF5 share target genes

329   **Figure S2:** BES1-BZR1-BEH family regulates seedling establishment during

330   photomorphogenesis in the presence of brassinosteroids.

331   **Figure S3:** BES1-BZR1-BEH family single loss-of-function mutants do not affect seedling

332   establishment during photomorphogenesis in the presence of picloram.

333   **Figure S4:** BZR1 contribution to auxin response in seedling stage.

334   **Figure S5:** Single loss-of-function of BES1 and BEH4 do not alter bipartite gene expression.

335   **Figure S6:** Bipartite elements are required for proper expression pattern and hormonal activation

336   of $XTH19_{PRO}$

337   **Table S1.** List of SAUR genes with bipartite elements.

338   **Table S2.** List and nucleotide sequence of primers used in this work.

339

340

341   **Figure legends**

342   **Figure 1. BES1 increases auxin sensitivity and DNA binding by ARF5.**

343   **(A)** Hypocotyl response of wild-type (WT) and *bes1-D* gain-of-function mutant seedlings to the

344   synthetic auxin picloram (PIC). Open symbols are seedlings exposed to control treatments, and

345   closed symbols are hormone treated samples. *bes1-D* was significantly taller than WT on D4-

346   under mock and treated conditions. *bes1-D* was significantly longer than WT on D4-8 Asterisks

347   indicate p value< 0.001 **(B)** Binding by ARF5 on several promoters was enhanced in *bes1-D*

348   mutants under mock condition. Bars represent the mean of four biological replicates.

349

350

351   **Figure 2. BEH4 acts redundantly with BES1 to regulate auxin and BR seedling responses.**

352   **(A)** 7-day-old seedling (upper panel) and 6-weeks rosette (lower panel) phenotype of wild-type,

353   *bin2-D, bes1-2 beh4*, *bes1-2* and *beh4-1* mutants grown in short day conditions. Hypocotyl

354   response of wild-type (WT) and *bes1-2 beh4-1* mutant seedlings to **(B)** brassinolide (BL) and **(C)**

355   picloram (PIC), grown as indicated in Figure1. Open symbols are seedlings exposed to control

356   treatments, and closed symbols are hormone treated samples. *bes1-2 beh4-1* was significantly

357   shorter than WT on D4-8 (p value< 0.01) under control and brassinolide, and only on D7-8 (p

358   value< 0.05) picloram conditions. WT and *bes1 beh4-1* control samples are the same and

359   repeated for reference in panel B and C.

360

361   **Figure 3. Expression of ARF5-BES1 targets is hormone sensitive and important for growth.**

362   **(A)** BES1 and BEH4 status affects the expression of ARF5 targets. RT-qPCR analysis of

363   bipartite target gene expression in 7-day-old seedlings without any treatment. The fold change

364   expression of *XTH19*, *IAA6*, *PIF7* and *LNG1* is shown in *bes1-D* and *bes1-2 beh4-1* double

365   mutants relative to WT. **(B)** Hormone responsiveness of target genes in WT under control

366   (mock), 3h of IAA or BL treatment. **(C)** Hormone responsiveness of target genes is altered in

367   *bes1-D* and *bes1-2 beh4-1* double mutant. Means of three biological replicates (relative

368   expression value normalized to housekeeping gene) is shown ± SE in A-C. **(D)** ARF5 target

369   genes are important for growth. Hypocotyl response of 7-day-old WT, *pif7-2*, *xth17* and *lng1-3*

370   mutant seedlings under control (mock), brassinolide (BL) or picloram (PIC) treatments. *:p

371   value< 0.05; ** :p value< 0.01 in comparisons between mock and treated samples in (B) and WT

372   vs. mutant phenotypes in (D).

373

374   **Figure 4. Other members of *XTH19* gene clade with bipartite promoter structure exhibit**

375   **similar hormone responsiveness in a BES1-dependent manner.**

376   **(A)** Promoter architecture of *XTH* genes. One kilobase upstream of the transcriptional start site is

377   shown. qPCR analysis of several *XTH* gene expression in 7-day-old seedlings in response to

378   control (mock), IAA or BL in **(A)** WT, **(B)** *bes1-D* and **(C)** *bes1-2 beh4-1* double mutant. Means

379   of three biological replicates (relative expression value normalized to housekeeping gene) is

380   shown ± SE. ** refers to p value< 0.01, * to p value< 0.05.

381

382   **Figure 5. Promoter architecture predicts hormone sensitivity.**

383   **Left panel:** Promoter architecture of non-bipartite *XTH* genes. One kilobase upstream of the

384   transcriptional start site is shown. **Right panel**: RT-qPCR analysis of selected non-bipartite *XTH*

385   gene expression in 7-day-old wild-type in response to 3h of control (mock), 50µM IAA or 1µM

386   BL (relative expression value normalized to housekeeping gene in WT). *: p value< 0.05 of

387   significant difference between treated and mock samples.

388

389   **Figure 6. ARF5-BES1-BEH4 transcriptional hub acts as a molecular switch to integrate**

390   **signals.**

391   Bipartite elements allow ARF5, BES1 and BEH4 to work together as a transcriptional module to

392   connect expression of a suite of growth-promoting genes to specific environmental conditions.

393

394 **References**

395   1.   de Wit M, Galvão VC, Fankhauser C. Light-Mediated Hormonal Regulation of Plant
396   Growth and Development. Annu Rev Plant Biol. 2016; doi:10.1146/annurev-arplant-
397   043015-112252

398   2.   Vaishak KP, Yadukrishnan P, Bakshi S, Kushwaha AK, Ramachandran H, Job N, et al.
399   The B-box bridge between light and hormones in plants. J Photochem Photobiol B Biol.
400   Elsevier B.V; 2019;191: 164–174. doi:10.1016/j.jphotobiol.2018.12.021

401   3.   Arsovski AA, Galstyan A, Guseman JM, Nemhauser JL. Photomorphogenesis. Arab B.
402   2012;10: e0147. doi:10.1199/tab.0147

403   4.   Chapman EJ, Estelle M. Mechanism of Auxin-Regulated Gene Expression in Plants. Annu
404   Rev Genet. 2009; doi:10.1146/annurev-genet-102108-134148

405   5.   Wang R, Estelle M. Diversity and specificity: Auxin perception and signaling through the
406   TIR1/AFB pathway. Current Opinion in Plant Biology. 2014.
407   doi:10.1016/j.pbi.2014.06.006

408   6.   Luo J, Zhou JJ, Zhang JZ. Aux/IAA gene family in plants: Molecular structure, regulation,
409   and function. Int J Mol Sci. 2018;19: 1–17. doi:10.3390/ijms19010259

410   7.   Guilfoyle TJ, Hagen G. Auxin response factors. Curr Opin Plant Biol. 2007; doi:S1369-
411   5266(07)00123-9 [pii]\r10.1016/j.pbi.2007.08.014

412   8.   Boer DR, Freire-Rios A, Van Den Berg WAM, Saaki T, Manfield IW, Kepinski S, et al.
413   Structural basis for DNA binding specificity by the auxin-dependent ARF transcription
414   factors. Cell. 2014; doi:10.1016/j.cell.2013.12.027

415   9.   Chandler JW. Auxin response factors. Plant Cell and Environment. 2016.
416   doi:10.1111/pce.12662

417   10. Galli M, Khakhar A, Lu Z, Chen Z, Sen S, Joshi T, et al. The DNA binding landscape of
418   the maize AUXIN RESPONSE FACTOR family. Nat Commun. Springer US; 2018;9:
419   4526. doi:10.1038/s41467-018-06977-6

420   11. Stigliani A, Martin-Arevalillo R, Lucas J, Bessy A, Vinos-Poyo T, Mironova V, et al.
421   Capturing auxin response factors syntax using DNA binding models. Mol Plant. 2018; 1–
422   11. doi:10.1016/j.molp.2018.09.010

423   12. Yin Y, Wang Z, Mora-garcia S, Li J, Yoshida S, Asami T, et al. BES1 Accumulates in the
424   Nucleus in Response to Brassinosteroids to Regulate Gene Expression and Promote Stem

425   Elongation. 2002;109: 181–191.

426 13. Yin Y, Vafeados D, Tao Y, Yoshida S, Asami T, Chory J, et al. A New Class of

427   Transcription Factors Mediates Brassinosteroid-Regulated Gene Expression in

428   Arabidopsis. 2005;120: 249–259. doi:10.1016/j.cell.2004.11.044

429 14. Li L, Deng XW. It runs in the family□: regulation of brassinosteroid signaling by the

430   BZR1 – BES1 class of transcription factors. 2005;10: 266–268.

431 15. Sun Y, Fan XY, Cao DM, Tang W, He K, Zhu JY, et al. Integration of Brassinosteroid

432   Signal Transduction with the Transcription Network for Plant Growth Regulation in

433   Arabidopsis. Dev Cell. 2010;19: 765–777. doi:10.1016/j.devcel.2010.10.010

434 16. Yu X, Li L, Zola J, Aluru M, Ye H, Foudree A, et al. A brassinosteroid transcriptional

435   network revealed by genome-wide identification of BESI target genes in Arabidopsis

436   thaliana. Plant J. 2011;65: 634–646. doi:10.1111/j.1365-313X.2010.04449.x

437 17. Li L. Brassinosteroids Stimulate Plant Tropisms through Modulation of Polar Auxin

438   Transport in Brassica and Arabidopsis. PLANT CELL ONLINE. 2005;

439   doi:10.1105/tpc.105.034397

440 18. Chaiwanon J, Wang ZY. Spatiotemporal brassinosteroid signaling and antagonism with

441   auxin pattern stem cell dynamics in Arabidopsis roots. Curr Biol. 2015;25: 1031–1042.

442   doi:10.1016/j.cub.2015.02.046

443 19. Nakamura A, Nakajima N, Goda H, Shimada Y, Hayashi K, Nozaki H. Arabidopsis Aux /

444   IAA genes are involved in brassinosteroid-mediated growth responses in a manner

445   dependent on organ type. 2006; 193–205. doi:10.1111/j.1365-313X.2005.02582.x

446 20. Hardtke CS. Transcriptional auxin-brassinosteroid crosstalk: Who's talking? BioEssays.

447   2007;29: 1115–1123. doi:10.1002/bies.20653

448 21. Nemhauser JL, Mockler TC, Chory J. Interdependency of brassinosteroid and auxin

449   signaling in Arabidopsis. PLoS Biol. 2004; doi:10.1371/journal.pbio.0020258

450 22. Vert G, Walcher CL, Chory J, Nemhauser JL. Integration of auxin and brassinosteroid

451   pathways by Auxin Response Factor 2. Proc Natl Acad Sci. 2008;105: 9829–9834.

452   doi:10.1073/pnas.0803996105

453 23. Cho H, Ryu H, Rho S, Hill K, Smith S, Audenaert D, et al. A secreted peptide acts on

454   BIN2-mediated phosphorylation of ARFs to potentiate auxin response during lateral root

455   development. Nat Cell Biol. Nature Publishing Group; 2013;16: 66–76.

456   doi:10.1038/ncb2893

457   24.   Han S, Cho H, Noh J, Qi J, Jung HJ, Nam H, et al. BIL1-mediated MP phosphorylation

458   integrates PXY and cytokinin signalling in secondary growth. Nat Plants. Springer US;

459   2018;4: 605–614. doi:10.1038/s41477-018-0180-3

460   25.   Hu Z, Lu SJ, Wang MJ, He H, Sun L, Wang H, et al. A Novel QTL qTGW3 Encodes the

461   GSK3/SHAGGY-Like Kinase OsGSK5/OsSK41 that Interacts with OsARF4 to

462   Negatively Regulate Grain Size and Weight in Rice. Mol Plant. Chinese Society for Plant

463   Biology; 2018; doi:10.1016/j.molp.2018.03.005

464   26.   Yoshimitsu Y, Tanaka K, Fukuda W, Asami T, Yoshida S, Hayashi K ichiro, et al.

465   Transcription of DWARF4 plays a crucial role in auxin-regulated root elongation in

466   addition to brassinosteroid homeostasis in arabidopsis thaliana. PLoS One. 2011;6.

467   doi:10.1371/journal.pone.0023851

468   27.   Chung Y, Maharjan PM, Lee O, Fujioka S, Jang S, Kim B, et al. Auxin stimulates

469   DWARF4 expression and brassinosteroid biosynthesis in Arabidopsis. Plant J. 2011;66:

470   564–578. doi:10.1111/j.1365-313X.2011.04513.x

471   28.   Sakamoto T, Morinaka Y, Inukai Y, Kitano H, Fujioka S. Auxin signal transcription factor

472   regulates expression of the brassinosteroid receptor gene in rice. Plant J. 2013;73: 676–

473   688. doi:10.1111/tpj.12071

474   29.   Oh E, Zhu JY, Bai MY, Arenhart RA ugust., Sun Y, Wang ZY. Cell elongation is

475   regulated through a central circuit of interacting transcription factors in the Arabidopsis

476   hypocotyl. Elife. 2014;3. doi:10.7554/eLife.03031

477   30.   Walcher CL, Nemhauser JL. Bipartite Promoter Element Required for Auxin Response.

478   PLANT Physiol. 2012;158: 273–282. doi:10.1104/pp.111.187559

479   31.   Schlereth A, Möller B, Liu W, Kientz M, Flipse J, Rademacher EH, et al.

480   MONOPTEROS controls embryonic root initiation by regulating a mobile transcription

481   factor. Nature. 2010;464: 913–916. doi:10.1038/nature08836

482   32.   Goda H, Sawa S, Asami T, Fujioka S, Shimada Y, Yoshida S. Comprehensive

483   Comparison of Auxin-Regulated and Brassinosteroid-Regulated Genes in Arabidopsis.

484   PLANT Physiol. 2004;134: 1555–73. doi:10.1104/pp.103.034736

485   33.   Lachowiec J, Mason GA, Schultz K, Queitsch C. Redundancy, feedback, and robustness

486   in the Arabidopsis thaliana BZR/BEH gene family. Front Genet. 2018;9: 053447.

487   doi:10.1101/053447

488   34.   Vissenberg K, Oyama M, Osato Y, Yokoyama R, Verbelen J, Nishitani K. Differential

489   Expression of AtXTH17 , AtXTH18 , AtXTH19 and AtXTH20 Genes in Arabidopsis

490   Roots . Physiological Roles in Specification in Cell Wall Construction. 2005;46: 192–200.

491   doi:10.1093/pcp/pci013

492   35.   Miedes E, Suslov D, Vandenbussche F, Kenobi K, Ivakov A, Straeten V Der, et al.

493   Xyloglucan endotransglucosylase / hydrolase (XTH) overexpression affects growth and

494   cell wall mechanics in etiolated Arabidopsis hypocotyls. J Evol Biol. 2013;64: 2481–

495   2497. doi:10.1093/jxb/ert107

496   36.   Sun N, Wang J, Gao Z, Dong J, He H, Terzaghi W, et al. Arabidopsis SAURs are critical

497   for differential light regulation of the development of various organs. 2016;113: 1–6.

498   doi:10.1073/pnas.1604782113

499   37.   Lachowiec J, Lemus T, Thomas JH, Murphy PJM, Nemhauser JL, Queitsch C. The

500   Protein Chaperone HSP90 Can Facilitate. 2013;193: 1269–1277.

501   doi:10.1534/genetics.112.148098

502   38.   Heggie L, Halliday KJ. The highs and lows of plant life: Temperature and light

503   interactions in development. International Journal of Developmental Biology. 2005.

504   doi:10.1387/ijdb.041926lh

505   39.   Zhang D, Ye H, Guo H, Johnson A, Zhang M, Lin H, et al. Transcription factor HAT1 is

506   phosphorylated by BIN2 kinase and mediates brassinosteroid repressed gene expression in

507   Arabidopsis. Plant J. 2014; doi:10.1111/tpj.12368

508   40.   Oh E, Zhu JY, Wang ZY. Interaction between BZR1 and PIF4 integrates brassinosteroid

509   and environmental responses. Nat Cell Biol. Nature Publishing Group; 2012;14: 802–809.

510   doi:10.1038/ncb2545

511   41.   Overvoorde PJ. Functional Genomic Analysis of the AUXIN/INDOLE-3-ACETIC ACID

512   Gene Family Members in Arabidopsis thaliana. PLANT CELL ONLINE. 2005;

513   doi:10.1105/tpc.105.036723

514   42.   Li L, Ljung K, Breton G, Schmitz RJ, Pruneda-Paz J, Cowing-Zitron C, et al. Linking

515   photoreceptor excitation to changes in plant architecture. Genes Dev. 2012;

516   doi:10.1101/gad.187849.112

517   43.   Kim BC, Soh MS, Kang BJ, Furuya M, Nam HG. Two dominant photomorphogenic

518   mutations of Arabidopsis thaliana identified as suppressor mutations of hy2. Plant J. 1996;

519   doi:10.1046/j.1365-313X.1996.09040441.x

520 44. Li L, Ljung K, Breton G, Li L, Ljung K, Breton G, et al. Linking photoreceptor excitation

521   to changes in plant architecture Linking photoreceptor excitation to changes in plant

522   architecture. 2012; 785–790. doi:10.1101/gad.187849.112

523 45. Drevensek S, Goussot M, Duroc Y, Christodoulidou A, Steyaert S, Schaefer E, et al. The

524   Arabidopsis TRM1-TON1 Interaction Reveals a Recruitment Network Common to Plant

525   Cortical Microtubule Arrays and Eukaryotic Centrosomes. Plant Cell. 2012;

526   doi:10.1105/tpc.111.089748

527 46. Lee YK, Kim G, Kim I, Park J, Kwak S, Choi G, et al. regulate longitudinal cell

528   elongation in Arabidopsis. 2006;4314: 4305–4314. doi:10.1242/dev.02604

529 47. Sapala A, Runions A, Routier-Kierzkowska AL, Gupta M Das, Hong L, Hofhuis H, et al.

530   Why plants make puzzle cells, and how their shape emerges. Elife. 2018;

531   doi:10.7554/eLife.32794

532 48. Chen X, Wu S, Liu Z, Friml J. Environmental and Endogenous Control of Cortical

533   Microtubule Orientation. Trends in Cell Biology. 2016. doi:10.1016/j.tcb.2016.02.003

534 49. Wu S-Z, Bezanilla M. Actin and microtubule cross talk mediates persistent polarized

535   growth. J Cell Biol. 2018; doi:10.1083/jcb.201802039

536 50. Robinson S, Kuhlemeier C. Global Compression Reorients Cortical Microtubules in

537   Arabidopsis Hypocotyl Epidermis and Promotes Growth. Curr Biol. 2018;

538   doi:10.1016/j.cub.2018.04.028

539 51. Wang X, Zhang J, Yuan M, Ehrhardt DW, Wang Z, Mao T. *Arabidopsis*

540   MICROTUBULE DESTABILIZING PROTEIN40 Is Involved in Brassinosteroid

541   Regulation of Hypocotyl Elongation. Plant Cell. 2012;24: 4012–4025.

542   doi:10.1105/tpc.112.103838

543 52. Sasidharan R, Keuskamp DH, Kooke R, Voesenek LACJ. Interactions between Auxin ,

544   Microtubules and XTHs Mediate Green Shade- Induced Petiole Elongation in

545   Arabidopsis. 2014;9: 1–13. doi:10.1371/journal.pone.0090587

546 53. Lanza M, Garcia-Ponce B, Castrillo G, Catarecha P, Sauer M, Rodriguez-Serrano M, et al.

547   Role of Actin Cytoskeleton in Brassinosteroid Signaling and in Its Integration with the

548   Auxin Response in Plants. Dev Cell. 2012; doi:10.1016/j.devcel.2012.04.008

549   54.   Lee YK, Rhee JY, Lee SH, Chung GC, Park SJ, Segami S, et al. Functionally redundant
550   LNG3 and LNG4 genes regulate turgor-driven polar cell elongation through activation of
551   XTH17 and XTH24. Plant Mol Biol. 2018; doi:10.1007/s11103-018-0722-0

552   55.   Hwang G, Zhu J-Y, Lee YK, Kim S, Nguyen TT, Kim J, et al. PIF4 Promotes Expression
553   of LNG1 and LNG2 to Induce Thermomorphogenic Growth in Arabidopsis. Front Plant
554   Sci. 2017; doi:10.3389/fpls.2017.01320

555   56.   Ibañez C, Delker C, Martinez C, Bürstenbinder K, Janitza P, Lippmann R, et al.
556   Brassinosteroids Dominate Hormonal Regulation of Plant Thermomorphogenesis via
557   BZR1. Curr Biol. 2018; doi:10.1016/j.cub.2017.11.077

558   57.   Li QF, Lu J, Yu JW, Zhang CQ, He JX, Liu QQ. The brassinosteroid-regulated
559   transcription factors BZR1/BES1 function as a coordinator in multisignal-regulated plant
560   growth. Biochim Biophys Acta - Gene Regul Mech. Elsevier; 2018;1861: 561–571.
561   doi:10.1016/j.bbagrm.2018.04.003

562   58.   Wang ZY, Nakano T, Gendron J, He J, Chen M, Vafeados D, et al. Nuclear-localized
563   BZR1 mediates brassinosteroid-induced growth and feedback suppression of
564   brassinosteroid biosynthesis. Dev Cell. 2002; doi:10.1016/S1534-5807(02)00153-3

565   59.   He J, Gendron JM, Yang Y, Li J, Wang Z. The GSK3-like kinase BIN2 phosphorylates
566   and destabilizes BZR1 , a positive regulator of the brassinosteroid signaling pathway in
567   Arabidopsis. 2002;99: 10185–10190.

568   60.   Leivar P, Monte E, Al-Sady B, Carle C, Storer A, Alonso JM, et al. The Arabidopsis
569   Phytochrome-Interacting Factor PIF7, Together with PIF3 and PIF4, Regulates Responses
570   to Prolonged Red Light by Modulating phyB Levels. PLANT CELL ONLINE. 2008;
571   doi:10.1105/tpc.107.052142

572   61.   Stewart Lilley JL, Gan Y, Graham IA, Nemhauser JL. The effects of DELLAs on growth
573   change with developmental stage and brassinosteroid levels. Plant J. 2013;76: 165–173.
574   doi:10.1111/tpj.12280

575   62.   Pfaffl MW. A new mathematical model for relative quantification in real-time RT-PCR.
576   Nucleic Acids Res. 2001;29: 45e–45. doi:10.1093/nar/29.9.e45

577   63.   Lilley JLS, Gee CW, Sairanen I, Ljung K, Nemhauser JL. An Endogenous Carbon-
578   Sensing Pathway Triggers Increased Auxin Flux and Hypocotyl Elongation. Plant Physiol.
579   2012;160: 2261–2270. doi:10.1104/pp.112.205575

580
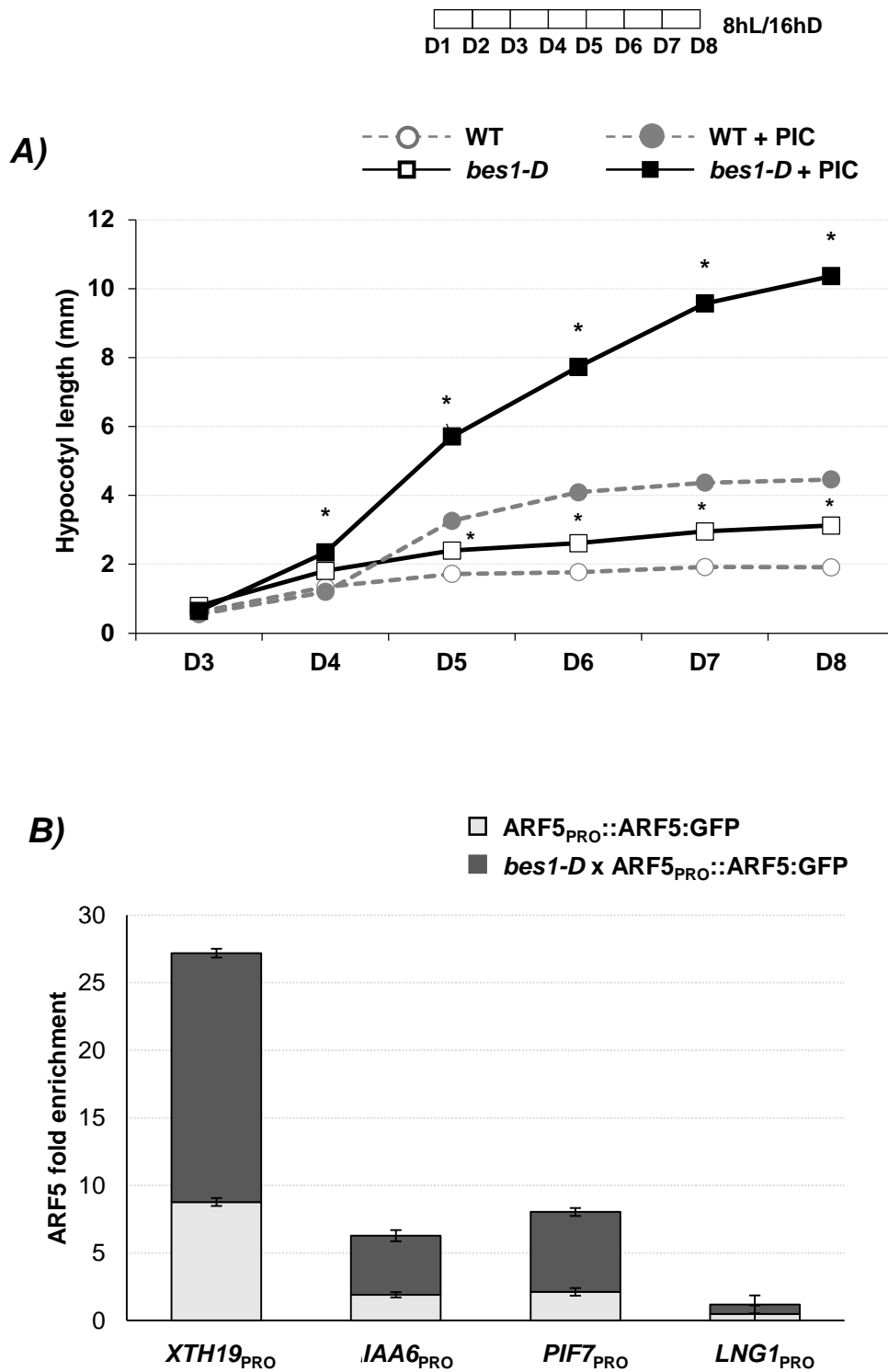
8hL/16hD

D1 D2 D3 D4 D5 D6 D7 D8

A)

B)

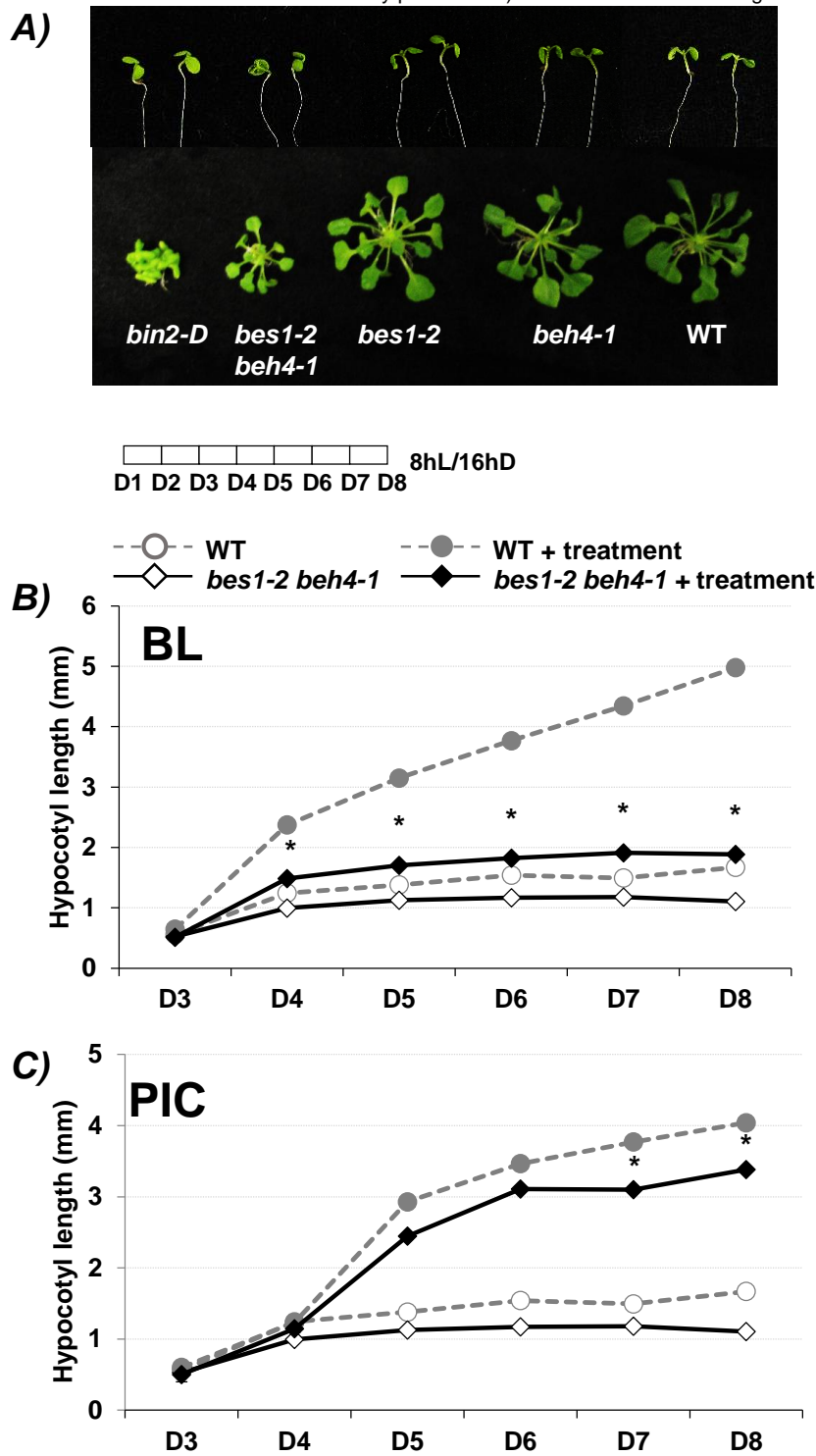**Figure 1. BES1 increases auxin sensitivity.**

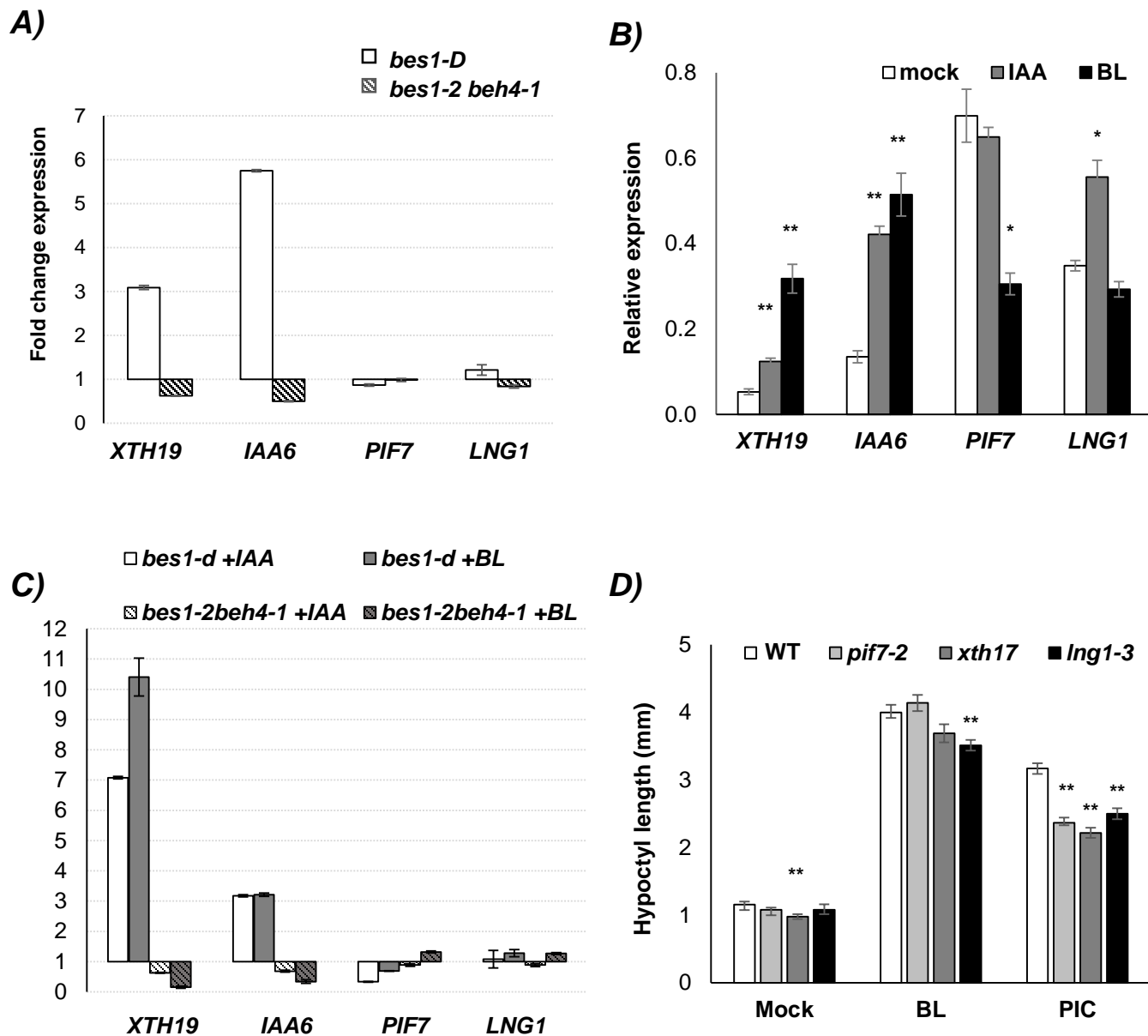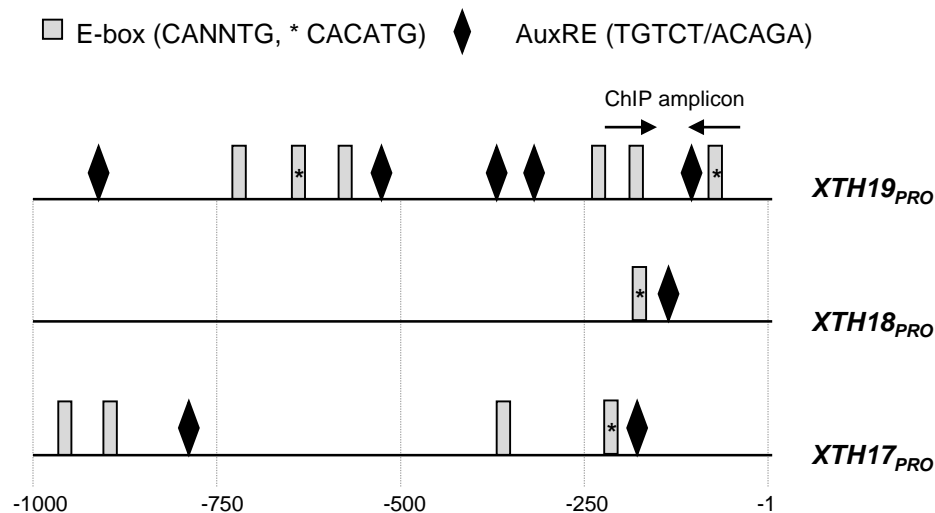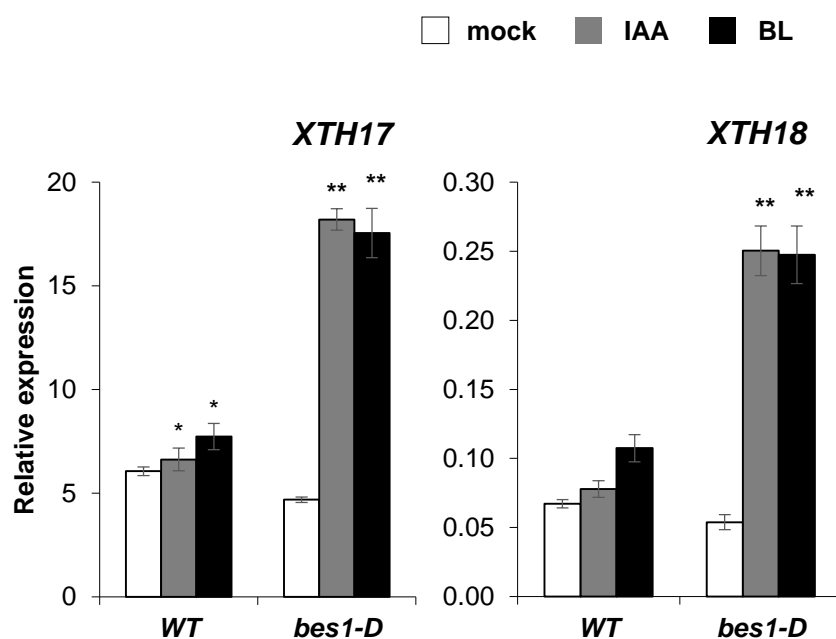**Figure 2. BEH4 acts redundantly to BES1 to regulate auxin and BR responses.**

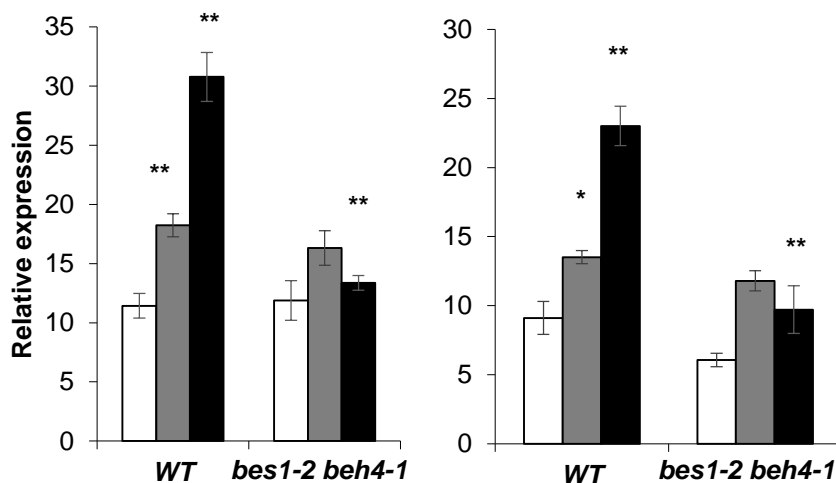**Figure 3 . Expression of ARF5-BES1 targets is hormone sensitive and important for growth.**

A)

☐ E-box (CANNTG, * CACATG)   ◆ AuxRE (TGTCT/ACAGA)

B)

C)

Figure 4. Other members of *XTH19* gene clade with bipartite promoter structure exhibit similar hormone responsiveness in a BES1-dependent manner.
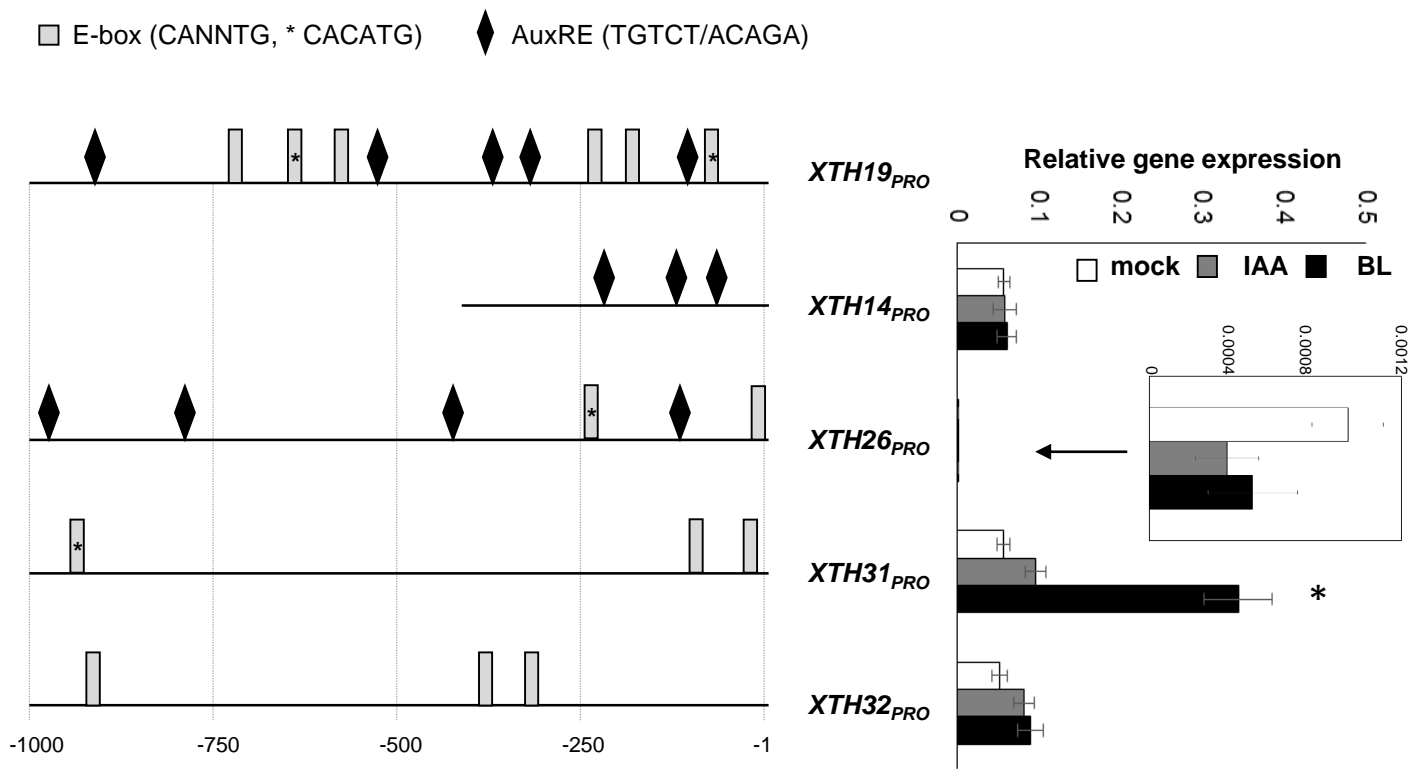
□ E-box (CANNTG, * CACATG)   ◆ AuxRE (TGTCT/ACAGA)

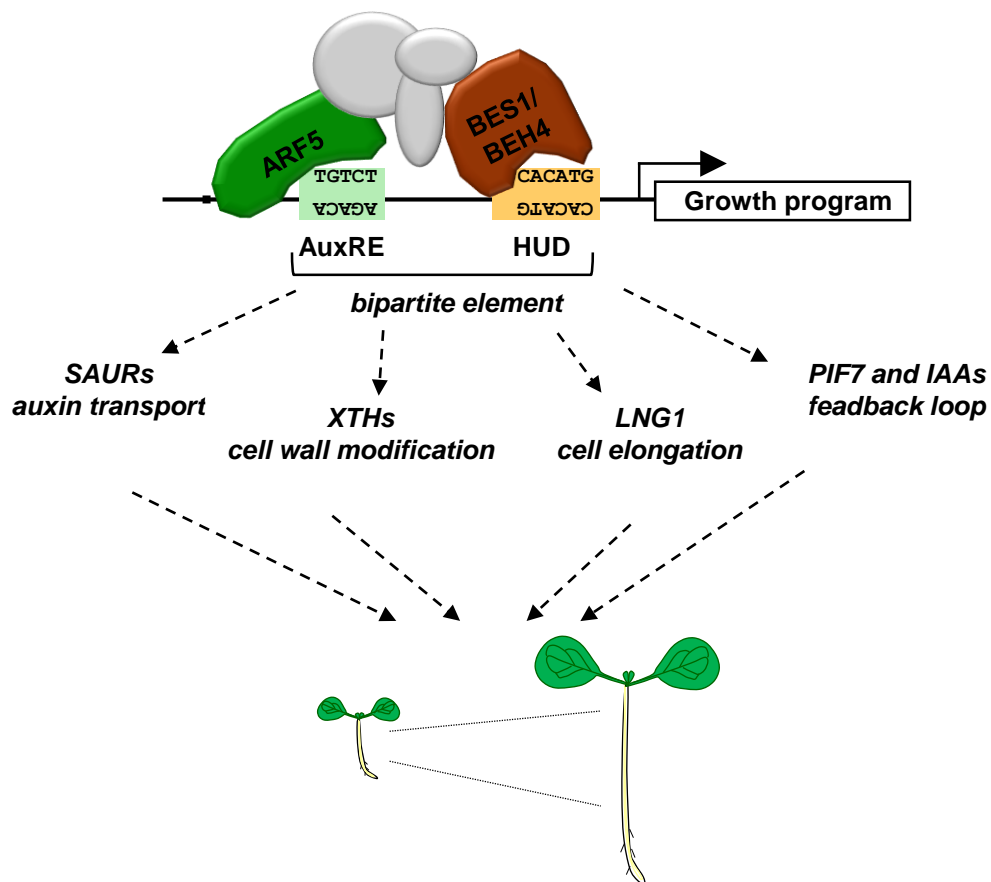**Figure 5. Promoter architecture predicts hormone sensitivity.**

Figure 6. ARF5-BES1-BEH4 transcriptional hub acts as a molecular switch to integrate signals.